Chemical Engineering Journal 156 (2010) 562–570

Contents lists available at ScienceDirect

Chemical Engineering Journal

journal homepage: www.elsevier.com/locate/cej

Preparation of titanium silicalite-1 catalytic films and application as catalytic membrane reactors

Xiaobin Wang[a], Xiongfu Zhang[a,*], Haiou Liu[a], King Lun Yeung[b], Jinqu Wang[a]

[a] State Key Laboratory of Fine Chemicals, School of Chemical Engineering, Dalian University of Technology, Dalian 116012, PR China
[b] Department of Chemical Engineering, The Hong Kong University of Science and Technology, Clear Water Bay, Kowloon, Hong Kong, SAR, PR China

ARTICLE INFO

Article history:
Received 14 January 2009
Received in revised form 1 April 2009
Accepted 1 April 2009

Keywords:
Zeolite
Film
TS-1
Silicalite-1
Catalytic membrane reactors

ABSTRACT

Titanium silicalite-1 (TS-1) films were prepared on porous α-Al_2O_3 tubes using nanosized silicalite-1 (Sil-1) particles as seeds by hydrothermal treatment and a TS-1 catalytic membrane reactors (CMR) was reasonably designed and evaluated by phenol hydroxylation with hydrogen peroxide as oxidant. Some factors on influencing TS-1 film formation and catalytic properties were investigated and the TS-1 films were characterized by scanning electron microscope (SEM), transmission electron micrograph (TEM), X-ray diffractometer (XRD), FTIR, UV–vis and X-ray fluorescence (XRF). It was indicated that TS-1 films prepared from Sil-1 and TS-1 seeds were comparable in structure, morphology and reaction behavior. The crystallization time and times of TS-1 film had a strong effect on its morphology, thickness and orientation. However, the film thickness could be easily controlled by crystallization time and times. The Ti/Si ratio in synthesis solution intensely influenced the content of the titanium atoms incorporated as framework Ti that was correlated well with the activity. The maximum Ti (IV) incorporated corresponds to a Ti/Si ratio of approximately 0.02–0.03. A constant conversion for phenol hydroxylation was obtained with the film thickness of over 7.5 μm. It is demonstrated that most of the reaction occurred in a shallow layer near the film due to the mass transfer effects in the TS-1 films.

1. Introduction

Since titanium silicalite-1 (TS-1) zeolite as oxidation catalyst was first synthesized by Taramasso et al. [1] in 1983, the TS-1 zeolite has become an important selective catalyst for oxidation of organic compounds using hydrogen peroxide under mild reaction conditions [2,3]. From these reactions, phenol hydroxylation and cyclohexanone ammoximation have been demonstrated on industrial scale. Most reaction studies were performed on TS-1 powder catalysts where the activity displays strong size dependence [4–7], but only a few reactions had been conducted on films or membranes [8–13]. TS-1 films and membranes were grown on monoliths [14–15] and other supports [16–18] by different methods including hydrothermal synthesis, sol–gel process and microwave method. Especially, microwave method has been received increasing attention in synthesis of zeolite and membrane during the past years because microwave synthesis not only reduces the synthesis time but also controls the morphology, orientation, composition and phase selectivity. Recently, microwave synthesis method has been utilized to fabricate the MFI crystals incorporating metal species [19] and MFI membranes [20,21]. Although support chemistry plays an important role in zeolite synthesis as shown by Au et al. [22], pre-seeding the support can significantly reduce their effects on zeolite deposition and growth as reported by Chau et al. [23]. Indeed, seeding is important in regulating zeolite growth [24] and could be used to control the film orientation [25–27] and morphology [28–30].

This paper investigates the preparation of TS-1 films on porous α-Al_2O_3 tubes using seeded secondary growth method. Supported TS-1 films grown from TS-1 and Si1-1 seeds were prepared and the influence of synthesis composition and condition on film growth, orientation and composition were studied. The zeolite films were examined by electron microscopy, X-ray diffraction, X-ray fluorescent spectroscopy, infrared and UV–vis spectroscopies and the catalytic activity TS-1 film was studied for phenol hydroxylation.

2. Experimental

2.1. Materials

The porous α-Al_2O_3 ceramic tubes supplied by the Nanjing University of Technology were used as support for the zeolite membrane. The outer and inner diameters of the tube are 13 mm and 10 mm, respectively. The ceramic tube prepared by sintering had a mean pore size of around 3 μm and a porosity of about 40%. The chemicals used for the zeolite synthesis included the

* Corresponding author. Tel.: +86 411 39893605; fax: +86 411 83633080.
E-mail address: xfzhang@dlut.edu.cn (X. Zhang).

1385-8947/$ – see front matter © 2009 Elsevier B.V. All rights reserved.
doi:10.1016/j.cej.2009.04.018

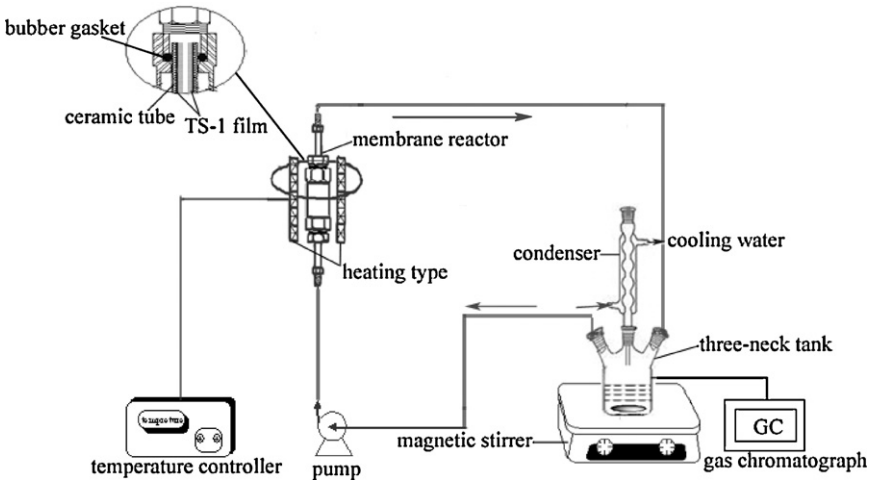

Fig. 1. Schematic of the reaction apparatus.

tetrabutyl orthotitanate (TBOT, 98.5%) from Beijing Xingjin Chemical Reagent Co. and tetraethyl orthosilicate (TEOS, 98%) from Tianjin Kermel Chemical Reagent Ltd. Co. The 17 wt.% tetrapropyl ammonium hydroxide (TPAOH) was synthesized in the laboratory. The reagents used for the phenol hydroxylation were purchased from Tianjian Kermel and included phenol (98.5%), benzene (99.5%), hydrogen peroxide (H_2O_2, 30%), acetone (ACE, 99.5%) and ethanol (99.7%).

2.2. Synthesis of TS-1 zeolite films

The 200 nm Sil-1 and TS-1 zeolite seeds were prepared according to the procedure reported in the literatures [6,31–33]. The Sil-1 seeds were obtained from a clear synthesis solution of 1 SiO_2: 0.22 TPA_2O: 19.2 H_2O after hydrothermal treatment at 398 K for 8 h, while the TS-1 seeds were obtained from 0.02 TiO_2: 1 SiO_2: 0.22 TPA_2O: 19.2 H_2O at 398 K and 8 h. The seeds were recovered and purified by a series of centrifugation and washing steps to remove coarse particles and unreacted gels and reagents. Final colloidal seed suspensions of 2 wt.% in water were obtained by dilution with deionized, distilled water. The support tube was cut to 75 mm lengths, cleaned by a series of sonication in acetone and distilled water to remove dirt and contaminants, and dried in an oven overnight at 393 K. The tube was seeded by dip-coating in the 2 wt.% colloidal seed suspension for 40 s to deposit a uniform seed layer on the inner surface of the tube.

The seeded tube was dried overnight at room temperature and calcined in air for 6 h at 823 K at a heating rate of 1 K min^{-1}. The heat treatment served to improve the adhesion of the seed layer by sintering the zeolite nanoparticles. The seeded tube was then wrapped with layers of Teflon tape to prevent zeolite deposition on the outer walls of tube during the synthesis, and immersed in the synthesis solution with a composition of 1 SiO_2: 0–0.05 TiO_2: 0.18 TPA_2O: 250 H_2O in a Teflon vessel. The vessel was sealed in a stainless steel autoclave and placed in a 448 K oven for zeolite film deposition. The synthesis solution was prepared by slowly adding TEOS to the TPAOH solution under vigorous mixing followed by the dropwise addition of dissolved TBOT in dry isopropanol. The mixture was slowly heated to 358 K in a water bath to evaporate the alcohols (i.e., alcohol, isopropanol and butanol). Deionized, distilled water was added to make up for the lost volume. The solution was aged 24 h at room temperature to obtain a clear synthesis solution.

2.3. Characterization of TS-1 films

Each step in the preparation of the TS-1 film on the porous ceramic support was examined by scanning electron microscope (SEM, KYKY-2800B). Samples were sectioned with wafering saw and mounted on specimen stabs with conducting adhesives. A thin

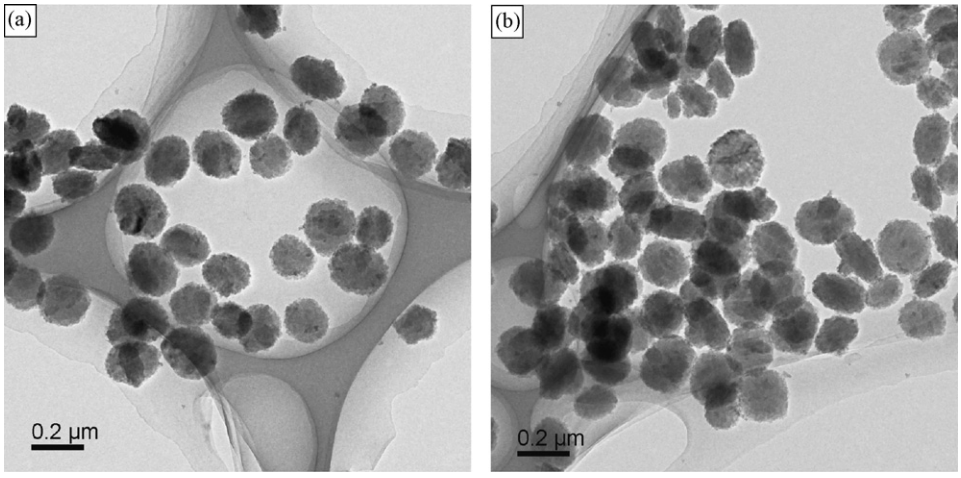

Fig. 2. The TEM of (a) Sil-1 and (b) TS-1 seeds.

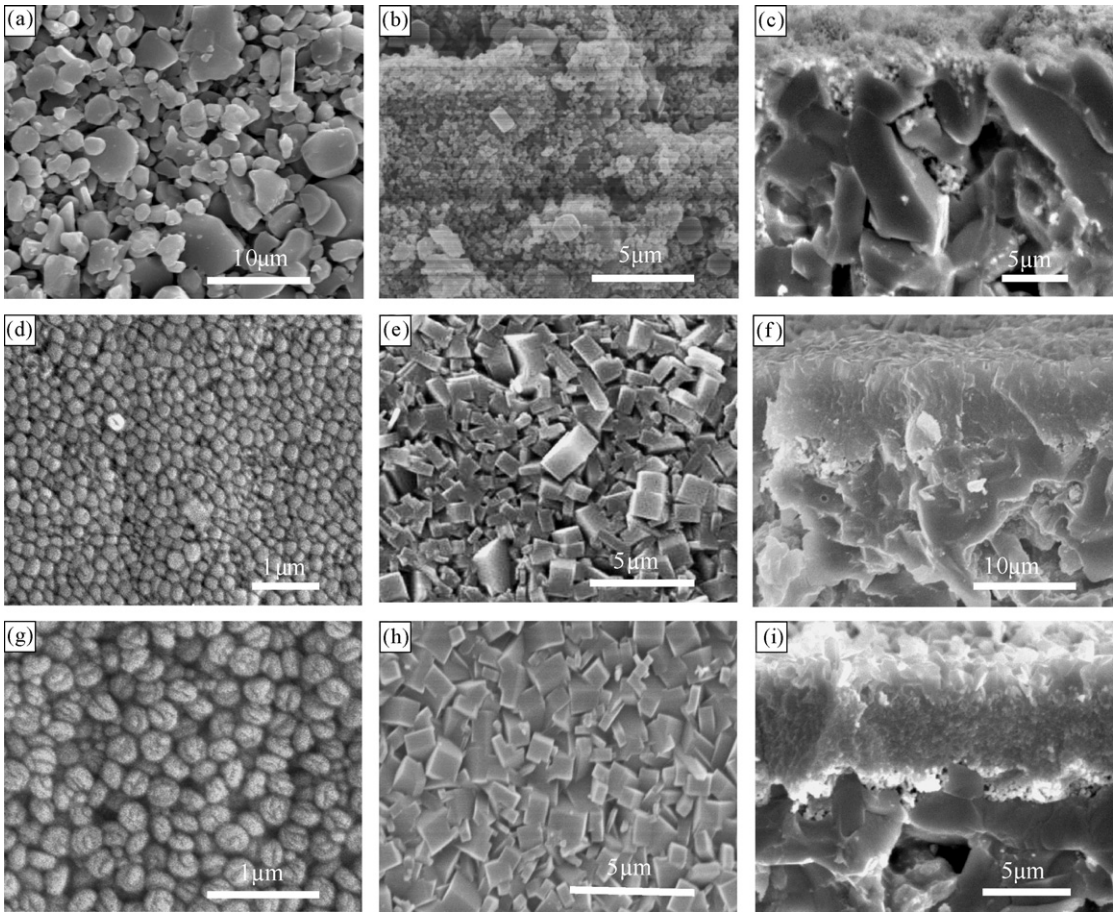

Fig. 3. SEM images of the samples. (a) Surface of the support; (b) and (c) TS-1 film without seeds; (d)–(f) seeded support and corresponding TS-1 film with TS-1 seed; (g)–(i) seeded support and corresponding TS-1 film with Sil-1 seed.

layer of gold was sputtered on the sample to decrease sample charging during imaging at 15 kV and 50 mA. The zeolite film orientation was determined by D/Max 2400 Rigaku X-ray diffractometer (XRD) with a Cu Kα radiation source (λ = 0.1542 nm), and operated at a voltage of 40 kV and 50 mA. The bulk composition of the TS-1 films was analyzed by the X-ray fluorescence spectrum (XRF, SRS3400). Spectroscopy techniques including infrared and UV–vis spectroscopies, were used to monitor the titanium in zeolite framework. The infrared spectra were collected from Bruker EQUINOX55 spectrometer and the diffuse reflectance UV–vis spectra were obtained on a JASCO V-550 spectrometer and the samples were the powder recovered from the vessel. The transmission electron micrograph (TEM) of zeolite seeds were on a Tecnai 20 microscope at an accelerating voltage of 200 kV.

2.4. Phenol hydroxylation reaction

A schematic drawing of the reactor set-up for phenol hydroxylation reaction is shown in Fig. 1. The ceramic tube with the supported TS-1 film was sealed in a stainless steel reactor using Viton O-rings. The reactor was wrapped with heating tape and kept at the reaction temperature of 358 K. Ten grams of phenol dissolved in 23 ml dry acetone was circulated to the reactor at a flow rate of 0.88 $cm^3\ min^{-1}$ from a reservoir kept at 358 K by a water bath. A water cooled condenser was used to prevent excessive liquid evaporation in the three necked flask. Once the flow and temperature reached steady-state, 4.2 ml hydrogen peroxide was added to start the reaction. This gave a starting reaction mixture a molar ratio 1 phenol: 0.5 H_2O_2: 3 ACE. Reaction samples were taken every hour and analyzed by a gas chromatograph (GC7890F, Shanghai Techcomp Limited) equipped with a capillary column (SE-30, l 50 m × Φ 0.32 mm × 0.5 μm) and flame ionization detector. A typical reaction lasted for six hours. Reaction comparison was made with TS-1 powder catalyst recovered from the bottom of vessel. The batch reaction was carried out with reflux with 1 phenol: 0.5 H_2O_2: 3 ACE and 38 mg TS-1 powder catalyst at 358 K. The catalyst was separated from the reaction mixture by centrifugation prior to analysis.

3. Results and discussion

3.1. TS-1 film synthesis

3.1.1. Effects of seeding

Seeding followed by regrowth is a popular method for zeolite film and membrane preparation. By providing nucleation sites, seeding shortens the induction time for zeolite deposition and growth resulting in faster film growth [23]. The seeds also control the zeolite-type grown on the seeded surface and its growth orientation [34]. It is common practice to use the same zeolite to seed the growth of the film and membrane, however sometimes this may be difficult. It is time consuming and expensive to prepare submicron-sized TS-1 seeds compared to Sil-1 seeds. A prior work by the authors [35] indicated that TS-1 films prepared from Sil-1 seed were comparable to the films prepared from TS-1 seeds. Both TS-1 films exhibited similar activity and selectivity for catalytic oxidation of styrene to phenylacetaldehyde.

The Sil-1 and TS-1 seeds are of comparable size and morphology as shown by the TEM micrographs in Fig. 2a and b, respectively. The

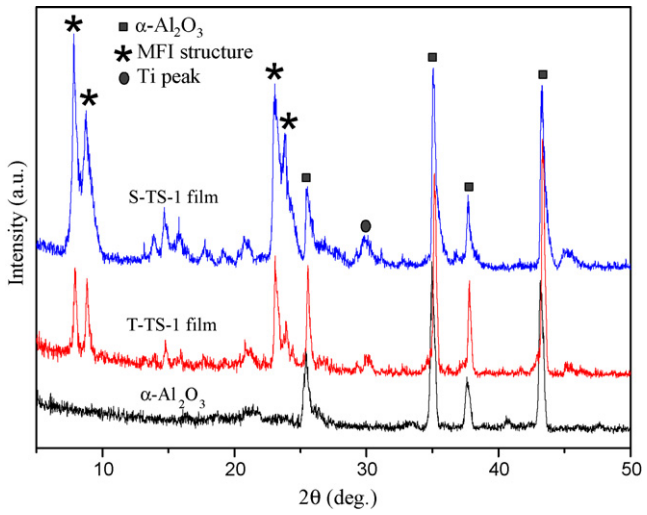

Fig. 4. XRD patterns of the support, TS-1 film with Sil-1 and TS-1 seeds, respectively.

TS-1 seeds had a Ti/Si ratio of 0.02 according to XRF. The surface of the ceramic support was imaged by scanning electron microscope and shown in Fig. 3a. The surface of the support was rough and consisted of sintered alumina particles of irregular size and shape. A mean pore diameter of 3 μm was measured, although larger pores were also evident from the micrograph. It was not possible to grow TS-1 film on the unseeded ceramic tube from the synthesis solution and conditions chosen for this work. It can be seen from the surface (Fig. 3b) and cross-section (Fig. 3c) that an amorphous gel layer had deposited on the ceramic. On the other hand, TS-1 films were successfully grown on both Sil-1 and TS-1 seeded tubes (Fig. 3e, f, h and i). The Sil-1 and TS-1 seeds deposited as a thin, uniform layer on the ceramic support as shown in Fig. 3d and g, respectively. Intergrown TS-1 films of comparable thickness of five microns were obtained from both seeds as shown by the SEM images. Fig. 4 shows that the TS-1 films also have similar X-ray diffraction pattern with the characteristic diffraction peaks of MFI structure (*d*-spacing = 11.2, 9.99, 3.8 and 3.7 for ⟨0 1 1⟩, ⟨0 2 0⟩, ⟨0 5 1⟩ and ⟨5 1 1⟩). The presence of a peak at (*d*-spacing = 3.04 for ⟨3 5 2⟩) is a good evidence of titanium incorporation in the zeolite framework. These results further support the previous findings that the TS-1 films prepared from Sil-1 and TS-1 seeds were comparable in structure and morphology.

3.1.2. TS-1 film growth

The growth of the TS-1 zeolite film on the Sil-1 seeded support was investigated and Fig. 5 plots the typical growth curve and the corresponding growth rate for the synthesis composition of 1 SiO_2: 0.02 TiO_2: 0.18 TPA_2O: 250 H_2O. The film thickness measured from the sample cross-sections and the mass of zeolite deposited are plotted in Fig. 5a as a function of synthesis time. The mass of the deposited zeolite was proportional to the film thickness from the SEM cross-sections. The film thickness obtained from SEM measurements, while the film thickness was divided by synthesis time to obtain average film growth. It is clear from the absence of the induction period in Fig. 5a that the zeolite growth on the seeded support is immediate. The growth rate accelerates during the first 36 h and reaches a maximum of 0.114 m h^{-1} as shown in Fig. 5b. Similar results were observed by Hedlund et al. [36,37] that the ZSM-5 film growth immediately on seeded support due to the seeds bypass the nucleation, while conventional method involved nucleation, deposition and crystallization [38]. The growth rate decreased as the reactants were consumed ($t > 36$ h). Thicker zeolite films were obtained by repeating the synthesis using fresh reactant mixtures.

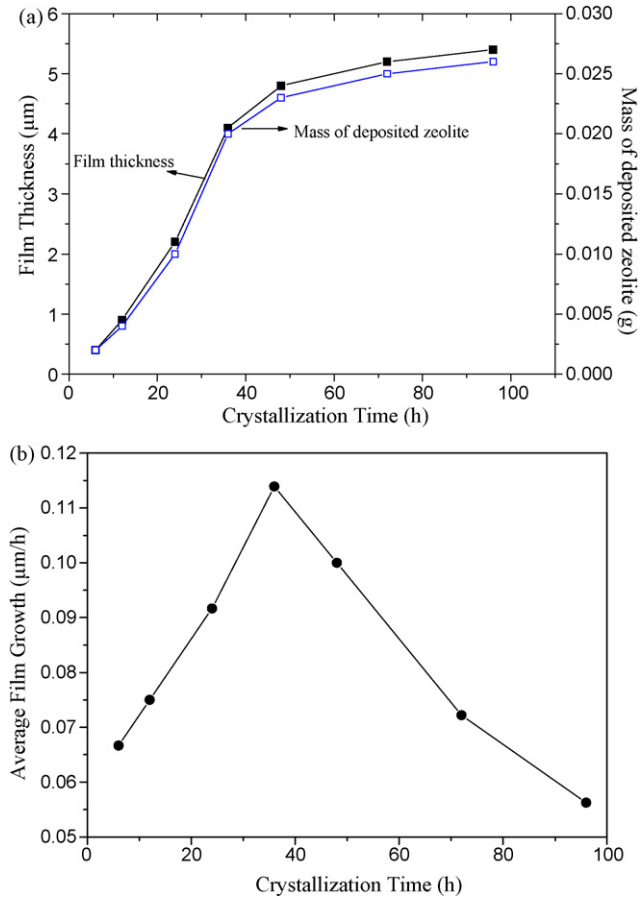

Fig. 5. The growth behavior of TS-1 films as a function of synthesis time: (a) film thickness and mass of deposited zeolite; (b) average film growth rate.

Fig. 6 plots the film thickness measured from the SEM cross-section and the mass increase following deposition. The TS-1 film growth was in nonlinear, while the ZSM-5 film growth was in linear [36] and the TS-1 film growth rate is lower than ZSM-5 film. This is maybe because the growth on substituted zeolite was slower due to the presence of the substituted framework metals and the reproducibility of the TS-1 film was not good. The zeolite growth study indicated that different thicknesses of TS-1 film could be grown on the Sil-1 seeded support.

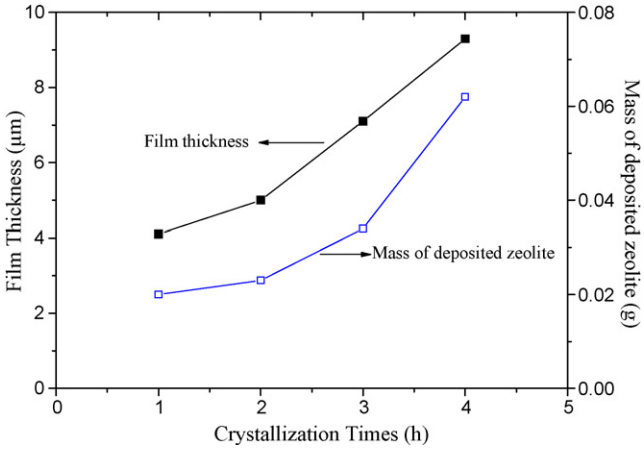

Fig. 6. The film thickness and mass of deposited zeolite as a function of synthesis times.

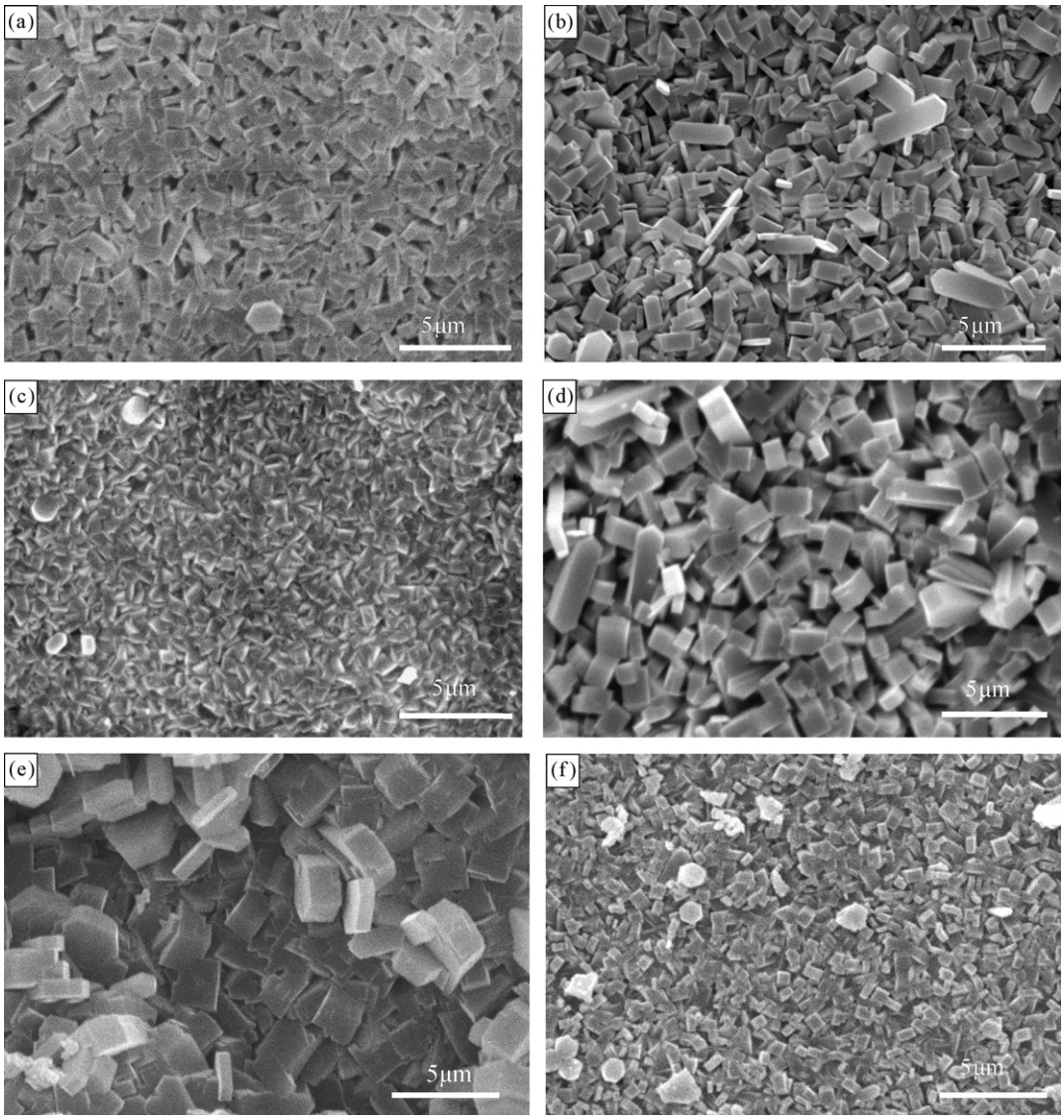

Fig. 7. Surface morphologies of the TS-1 films obtained at different synthesis time. (a) 12 h; (b) 24 h; (c) 48 h; and at different synthesis times of (d) 2; (e) 3; (f) 4.

The SEM observation indicated that zeolite film morphology and orientation evolved during the synthesis. Fig. 7 displays the representative SEM images obtained during early stages of zeolite growth (t = 12–48 h) (Fig. 7a–c) and after repeated regrowth of 2, 3 and 4 times (Fig. 7d–f). It can be seen from the micrograph that at early stage, the deposited zeolites have random orientation as the growth conformed to the rough support surface. The film roughness diminishes as the zeolite grows and smooth, intergrown, polycrystalline zeolite films are obtained as shown in Fig. 7c. The zeolite films obtained by repeated regrowth appear rougher than the previous film (Fig. 7d–f). It is speculated that this could be caused by the deposition of solution crystallized zeolite on the prior grown film that were not removed by the washing steps. These zeolites could increase the surface roughness by providing competing sites for zeolite growth. The X-ray diffraction data in Fig. 8 also indicates gradual change in the orientation of the deposited zeolite films with time and repeated regrowth in agreement with the SEM observation. The plots of the relative intensity of $I_{(011)}/I_{(051)}$, $I_{(511)}/I_{(051)}$, $I_{(020)}/I_{(051)}$ and $I_{(020)}/I_{(352)}$ with time is shown in Table 1. It is clear from Fig. 8 and Table 1 that the film orientation gradually changes from random to preferred ⟨0 2 0⟩ orientation. It also indicated that the titanium contents increased with increasing synthesis times.

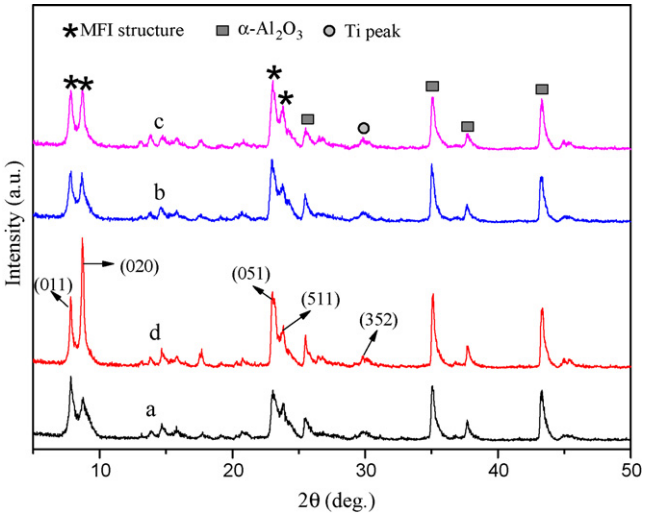

Fig. 8. XRD patterns of the TS-1 films with different crystallization time. (a) 12 h; (b) 24 h; (c) 48 h; (d) 72 h.

Table 1
Film orientation change with crystallization time.

Crystallization time (h)	$I_{(011)}$	$I_{(020)}$	$I_{(051)}$	$I_{(511)}$	$I_{(352)}$
12	113	89.1	100	89.5	14.6
24	93.4	93.8	100	93.0	56.8
48	96.2	96.8	100	95.6	85.0
72	83.3	126	100	82.1	85.4

The peak intensity (I_{051}) of (0 5 1) face is designed to 100, the peak intensities of other face are calculated by dividing actual intensity of (0 5 1) face.

3.1.3. Titanium incorporation

The titanium in the synthesis solution could be incorporated either as framework titanium atom in the TS-1 or extra-framework titanium and titanium dioxide deposits, and would have an important implication on the zeolite reactivity and selectivity. Although works investigating the effects of different synthesis parameters on the insertion of titanium atoms in the zeolite framework had been reported [39,40], their usefulness for TS-1 film preparation is limited due to the large difference in synthesis composition and conditions. Fig. 9a and b respectively display the infrared and UV–vis spectra of TS-1 films prepared from synthesis solution containing x TiO_2/SiO_2 of 0.01–0.05. The FTIR spectra of the TS-1 films display the characteristic bands for MFI zeolite at 1220 cm^{-1}, 1100 cm^{-1}, 800 cm^{-1}, 550 cm^{-1} and 450 cm^{-1}. The infrared signal at about 965 cm^{-1} is commonly agreed to originate from Ti–O–Si and often taken as indication of titanium substitution in the zeolite framework. The I_{965}/I_{800} ratio was used by Serrano et al. [41] as a measure of the titanium content in zeolite. Fig. 9c plots the I_{965}/I_{800} ratio for the different titanium content of the synthesis solution. A maximum was observed at x TiO_2/SiO_2 of around 0.02.

The UV–vis spectra (Fig. 9b) of the TS-1 film display a signal at 210 nm attributed to tetra-coordinated titanium [42]. The absence of the absorption band at the wavelength of 270–280 nm indicates that no hexa-coordinated titanium species is present in the samples [43]. However, anatase TiO_2 is clearly present in samples with x TiO_2/SiO_2 above 0.03 as a signal around 330 nm existence [44]. The plot of the I_{965}/I_{800} ratio in Fig. 9c clearly shows a decreasing trend above $x = 0.03$. Finally, a plot of y TiO_2/SiO_2 measured by X-ray fluorescent spectroscopy in Fig. 10 shows that the titanium content of the TS-1 films displays a similar maximum at the infrared data for I_{965}/I_{800} ratio at $x = 0.02$. This is according with the literatures which reported the maximum Ti (IV) incorporated into the TS-1 framework corresponds to a Ti/Si ratio of approximately 0.02–0.03 [45–47].

3.2. Phenol hydroxylation reaction

There are many reports [48–51] on the use of TS-1 zeolite as catalyst for phenol hydroxylation reaction to hydroquinone and catechol as shown in the reaction Scheme 1. In this reaction, dihydroxybenzenes and benzoquinone are the desired product and byproduct. Although not as widely studied, reactions on TS-1 films had been reported by several authors [35,52,53]. This includes our recent report on the reaction of styrene to phenylacetaldheyde over TS-1 film catalyst [35]. TS-1 film catalysts prepared from Sil-1 and TS-1 seeds exhibited similar reaction performance and phenylacetaldehyde selectivity increased with in-framework titanium content. The 1-pentene epoxidation reaction [52–54] and selective oxidation of aniline to azoxybenzene [55,56] were carried out in miniature reactors coated with TS-1 film catalyst.

3.2.1. Seeds and substrate

The phenol hydroxylation reaction was conducted on the porous alumina tube and Sil-1 seeded tube and trace conversions of 0.19% and 0.21% were observed for the respective tubes. It is therefore possible to conclude that both the porous alumina tube and Sil-1 seeds are inactive for the reaction. The phenol hydroxylation reaction was also investigated for TS-1 films grown from Sil-1 and TS-1 seeded ceramic tubes and the results are summarized in Table 2. The TS-1 films grown from 1 SiO_2: 0.02 TiO_2: 0.18 TPA_2O: 250 H_2O at 448 K for 48 h display similar comparable in structure and morphology as shown in Figs. 2 and 3. The 4.0 μm thick films weigh 20 mg and have Ti/Si ratio of 0.197 according to XRF. Table 2 shows that the two TS-1 films exhibit very similar reaction behavior regardless of the precursor seeds. The reaction conversion increases with reaction time and the selectivity to dihydroxybenzenes increases with time with benzoquinone as the main reaction byproduct. The hydroquinone-

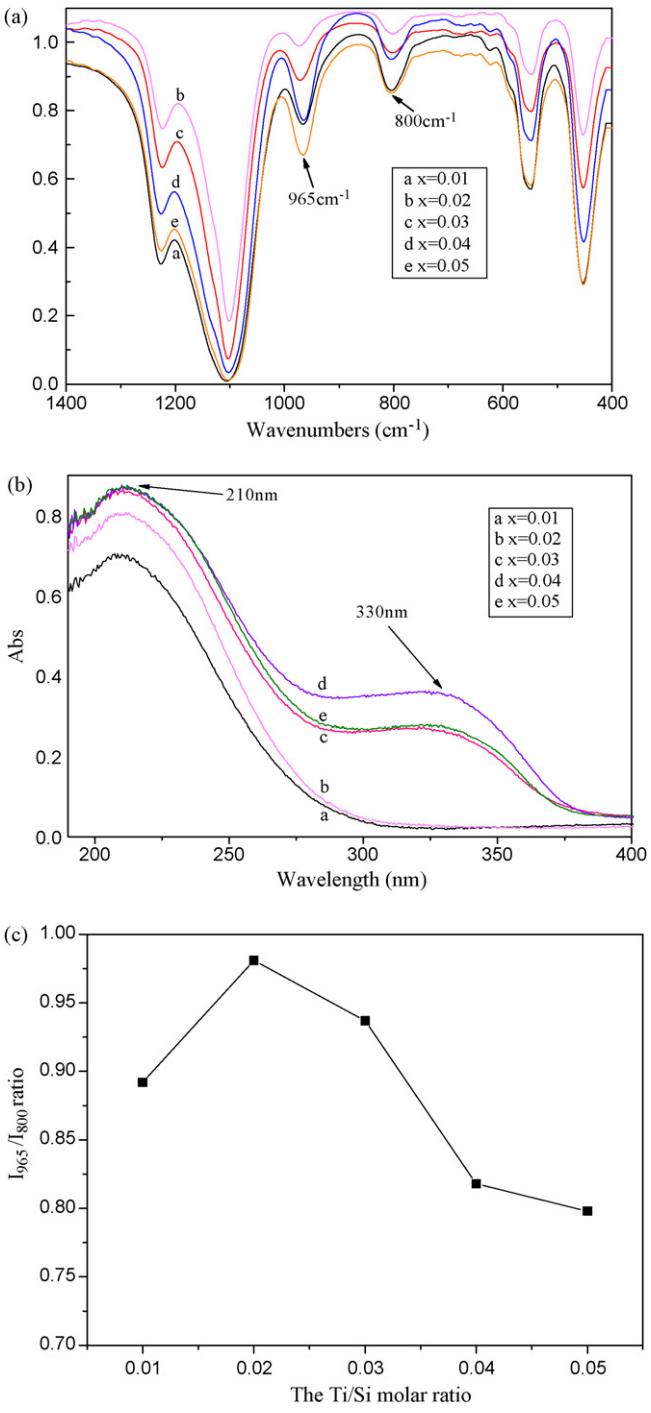

Fig. 9. The FT-IR (a), UV–vis (b) spectra and I_{965}/I_{800} ratio (c) of the TS-1 films synthesized with different Ti/Si ratios.

Table 2
The catalytic performances of TS-1 films with different seeds.

Reaction Time (h)	S–TS–1			T–TS–1		
	X_{Ph} (%)	S_{Di} (%)	HQ:CAT	X_{Ph} (%)	S_{Di} (%)	HQ:CAT
1	2.63	85.0	0.05	2.83	86.9	0.10
2	4.19	88.8	0.08	4.52	89.8	0.11
3	5.80	93.3	0.12	5.14	91.5	0.19
4	6.69	97.2	0.32	6.49	91.4	0.40
5	8.56	95.9	0.43	8.31	93.8	0.46
6	10.1	96.3	0.50	10.2	95.6	0.51

S–TS–1: TS-1 films with Sil-1 seeds; T–TS–1: TS-1 films with TS-1 seeds; X_{Ph}(%): phenol conversion; S_{Di}(%): dihydroxybenzenes selectivity; HQ:CAT: the hydroquinone-to-catechol molar ratio.

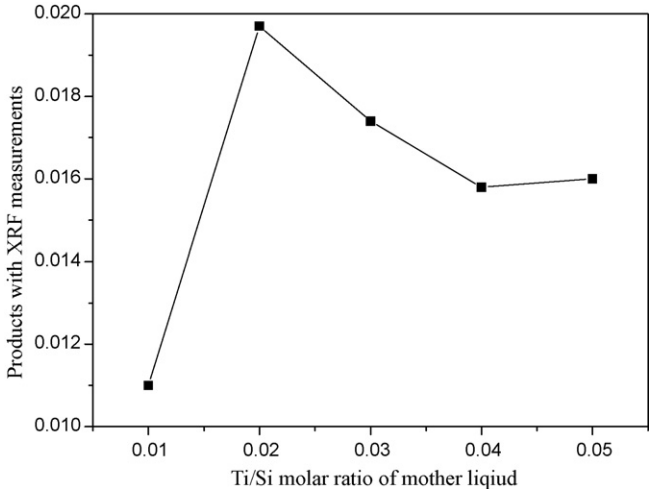

Fig. 10. The Ti/Si molar ratio of mother liquid ('x') and TS-1 Films according to XRF.

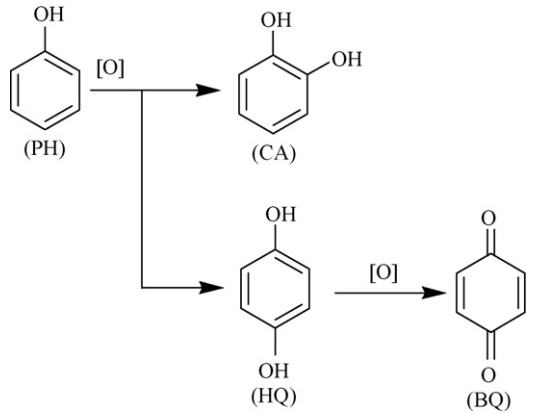

Scheme 1. Oxidation of phenol with hydrogen peroxide.

to-catechol ratio increases sharply after fourth hour of reaction. The change trend is similar to the literatures [48,57,58]. Thus, the initial fear that the Sil-1 seeds could lead to a dilution of the titanium content of the prepared TS-1 film and possible nonuniformity and maldistribution of zeolite composition resulting in poorer reaction performance is shown to be unfounded.

The ceramic support tube is a reservoir of impurities including aluminum, various alkali and alkaline earth metals that could contaminate the TS-1 film during the film synthesis. Aluminum could inhibit titanium incorporation and impart unwanted acidity to the prepared zeolite film [59–61]. Furthermore, trace amounts of alkali can effectively render TS-1 inactive [62,63]. Although TS-1 was less sensitive to alkaline earth [64,65], there present could affect film growth and orientation. Therefore, a reaction comparison was made between a supported 7.9 μm thick TS-1 film (38 mg) and a TS-1 powder catalyst (38 mg) as shown in Table 3. The TS-1 film was prepared from 1 SiO_2: 0.02 TiO_2: 0.18 TPA_2O: 250 H_2O at 448 K for 48 h through the same synthesis of three times and a Ti/Si ratio = 0.02. While the TS-1 powder collected from the bottom of the vessel with the Ti/Si ratio 0.02 and particle size approximately 400 nm. The film and the powder catalysts gave comparable phenol conversions of 14.8% and 14.4% for a reaction time of 6 h. Both catalysts gave selectivity to dihydroxybenzenes of 96%. However, the TS-1 film is more selective to catacheol compared to the powder catalyst (i.e., HQ/CAT ratio of 0.51 vs. 0.93). It is possible to conclude from the reaction results that impurities originating from the substrate appear not to significantly affect the activity and general selectivity of the catalyst to dihydroxybenzenes. It is believed that the difference in product distribution between film and powder catalysts is more due to mass transfer effects rather than reaction kinetics. The limited geometric area of the TS-1 film made access to the internal catalyst area of the film difficult and therefore it is expected that most of the reaction occurred in a shallow layer near the film surface. Indeed, it had been established by previous researchers that catechol is preferentially formed on the surface of TS-1 crystals [66] and this could explain the higher catechol yield from TS-1 film.

Table 3
The catalytic performances of TS-1 films with different Ti/Si molar ratio and thickness.

				X_{Ph} (%)	S_{Di} (%)	HQ:CAT
Nominal Ti/Si molar ratio (x)	0.01	Ti/Si molar ratio according to XRF	0.0110	10.3	99.2	0.47
	0.02		0.0197	12.4	99.2	0.47
	0.03		0.0174	7.26	87.3	0.50
	0.04		0.0158	6.09	86.2	0.46
	0.05		0.0162	3.76	84.2	0.42
TS-1 film thickness (μm) (x = 0.02)	2.2	TS-1 catalyst weight (mg)	10	6.79	99.9	0.47
	3.9		19	10.1	99.5	0.50
	4.5		22	13.5	98.1	0.46
	7.5		36	14.7	97.2	0.51
	7.9		38	14.8	96.1	0.51
	10		67	14.9	96.1	0.52
Mass of TS-1 powders		38 mg		14.4	96.5	0.93

X_{Ph} (%): phenol conversion; S_{Di} (%): dihydroxybenzenes selectivity; HQ:CAT: the hydroquinone-to-catechol molar ratio, reaction time: 6 h.

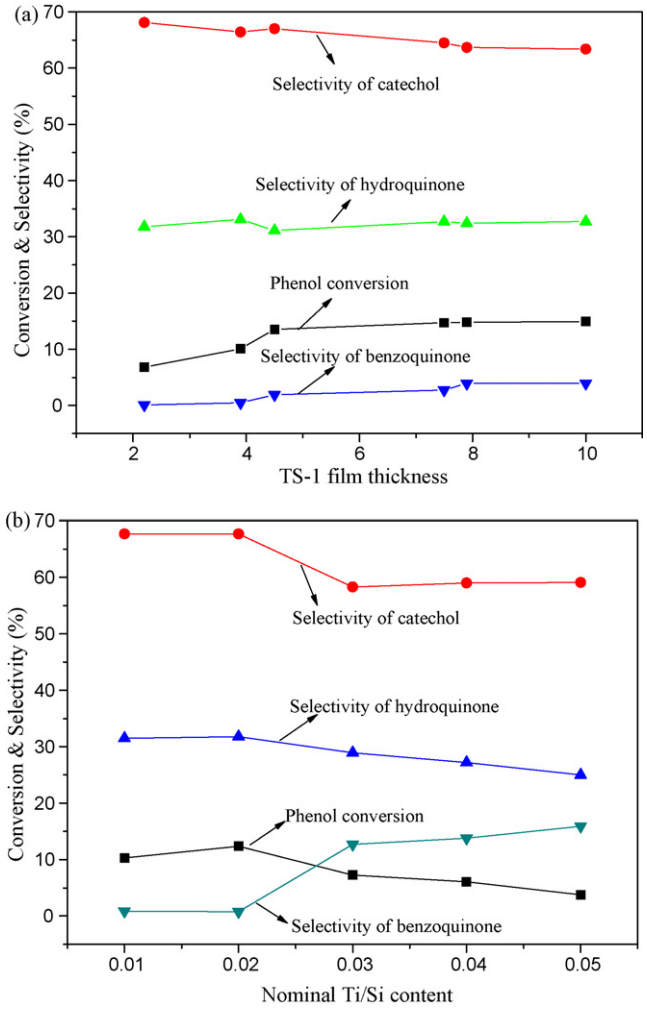

Fig. 11. Reaction conversion and product distribution as a function of different film thickness (a) and normal Ti/Si molar ratio (b).

3.2.2. TS-1 film thickness and nominal Ti/Si ratio

Fig. 11a plots the reaction conversion and product distribution for phenol hydroxylation reaction over a series of TS-1 films of different thicknesses. The reaction results are also summarized in Table 3. The plot shows that conversion increases with the film thickness reaching a plateau above film thickness of 7.5 μm. The mass of the catalyst increases in proportion to the deposited film thickness and therefore an increased catalyst activity is reasonable. The small interfacial area of the TS-1 film and the inherently slow diffusion of reactants and products in the zeolite pores rendered the catalysts below the depth of 7.5 μm inaccessible to the reaction. Therefore, a constant conversion is obtained for TS-1 films thicker than 7.5 μm, despite the higher catalyst mass.

Fig. 11b also plots the effects of the nominal Ti/Si content of the synthesis solution on the phenol conversion and product distribution. Fig. 10 shows the Ti/Si content of the TS-1 films display a nonlinear relationship with the nominal Ti/Si content of the synthesis solution. The phenol conversion correlates well with the films' Ti/Si ratio. The TS-1 films with high in-framework titanium content are more active as well as selective for dihydroxybenzenes production as reported in our previous work [35]. The lower reactivity and selectivity for TS-1 films prepared from solution with high Ti/Si content is due to the presence of anatase TiO_2 that could catalyze the decomposition of hydrogen peroxide and over-oxidation of phenol to benzoquinone. The results showed that the catalytic membrane reactors (CMR) reduced the intrinsic and external diffusion resistance compared to the TS-1 powder catalyst. Future work will focus on improving the activity of TS-1 CMR by optimizing the design and operation conditions of membrane reactor.

Table 4
The catalytic properties of TS-1 films with reaction times.

Reaction times	X_{Ph} (%)	S_{Di}(%)	HQ:CAT
1	13.7	98.1	0.47
2	10.1	90.6	0.45
3	9.26	85.5	0.40
4	6.25	80.4	0.37
5	6.01	73.7	0.37
After calcinations	13.2	98.9	0.47

X_{Ph} (%): phenol conversion; S_{Di} (%): dihydroxybenzenes selectivity; S_{BQ}: benzoquinone selectivity; HQ:CAT: the hydroquinone-to-catechol molar ratio, each reaction time: 6 h.

3.3. TS-1 deactivation and regeneration

A series of reaction runs was performed to investigate the deactivation and regenerability of the TS-1 film. The TS-1 film was prepared from 1 SiO_2: 0.02 TiO_2: 0.18 TPA_2O: 250 H_2O at 448 K for 48 h, and have a film thickness of 4.8 μm (23 mg) and Ti/Si ratio = 0.0197. The reaction results are displayed in Table 4 for five successive reactions each lasting 6 h. The TS-1 film was backwashed with deionized distilled water to remove the surface dirt and contaminants adsorbed reactants and products between runs. The phenol conversion decreased from 13.7% to 6.01% over the five runs (i.e., total reaction time of 30 h), and the dihydroxybenzenes desired product decreased from 98.1% to 73.7%. The poorer activity and selectivity are believed to be due to adsorbed reactants and byproducts in the zeolite pores that hindered the reaction and diffusion in the zeolite pore leading to phenol over-oxidation to benzoquinone. The original activity and selectivity was fully recovered once the TS-1 film was calcined at 823 K to remove the adsorbed impurities as shown in table.

4. Concluding remarks

In this work, the TS-1 films on both Sil-1 and TS-1 seeded tubes were prepared and compared in property. Also this paper first investigated the effects of synthesis parameters on the insertion of titanium atoms in the TS-1 film framework. The two TS-1 films were comparable in structure, morphology and reaction behavior regardless of the precursor seeds. TS-1 film growth rate seems to be slower than the ZSM-5 film due to the presence of the substituted metals in the synthesis solution. The synthesis time and times played important roles in the formation of TS-1 film and could easily adjust desired TS-1 film thickness. The framework titanium content of the TS-1 films reached maximum when the Ti/Si ratio of mother liquid was 0.02. The substrate and Sil-1 seeds appeared not to significantly affect the activity. The reaction mainly occurred in a shallow layer near the film surface, which leads to the catechol preferentially formed due to mass transfer effects rather than reaction kinetics. Thus, the film thickness had a slight effect on the reaction conversion, unlike on the use of TS-1 powder as catalyst. The conversion kept constant when the film thickness was over 7.5 μm due to the inherently slow diffusion of reactants and products in the zeolite pores rendered the catalysts below the depth of 7.5 μm inaccessible to the reaction. The dihydroxybenzenes production increased with increasing framework titanium content, while the lower reactivity and selectivity for TS-1 films with the films Ti/Si ratio exceeded 0.02 due to the presence of anatase TiO_2. The TS-1 films could be reused several times after simple treatment.

Therefore, future work will concentrate on improving the reaction conversion of TS-1 film CMR. One way is to make TS-1 films

grow on hollow fibers and structured supports to increase the geometric area of the catalyst. This can reduce the external and intrinsic diffusion resistance. Another is to introduce TS-1 film into a microreactor as CMR. A microreactor could enhance reaction performance due to eliminate the external mass transfer and rapid heat and mass transfers [11,13,67,68]. It is desirable to control the degree of crystal intergrowth during crystallization to obtain rougher catalyst film. This also favors improving faster diffusion by changing the surface structure of the catalyst. Further study on mechanism, modelling and other details is under way.

Acknowledgements

The authors gratefully acknowledge financial support provided by National Natural Science Foundation of China (Grant No. 20673017), PetroChina Innovation Fundation (Grant No. 2008D-5006-05-06) and China National 863 Program (Grant No. 2007AA05Z137).

References

[1] M. Taramasso, G. Perego, B. Notari, US Patent, 44 10 501 (1983).
[2] B. Notari, Catal. Today 18 (1993) 163–172.
[3] G. Bellussi, M.S. Rigutto, Stud. Surf. Sci. Catal. 85 (1994) 177–213.
[4] A.J.H.P. Van der Pol, A.J. Verduyn, J.H.C. van Hooff, Appl. Catal. A: Gen. 92 (1992) 113–130.
[5] A. Tuel, Y. Ben Taarit, Appl. Catal. A: Gen. 102 (1993) 69–77.
[6] G.Y. Zhang, J. Sterte, B.J. Schoeman, Chem. Mater. 9 (1997) 210–217.
[7] J. Ozaki, K. Takahashi, M. Sato, A. Oya, Carbon 44 (2006) 1243–1249.
[8] E.E. McLeary, J.C. Jansen, F. Kapteijn, Micropor. Mesopor. Mater. 90 (2006) 198–220.
[9] R. Dittmeyer, V. Hollein, K. Daub, J. Mol. Catal. A 173 (2001) 135–184.
[10] K.L. Yeung, R. Aravind, R.J.X. Zawada, J. Szegner, G. Cao, A. Varma, Chem. Eng. Sci. 49 (1994) 4823–4838.
[11] X.F. Zhang, E.S.M. Lai, R. Martin-Aranda, K.L. Yeung, Appl. Catal. A: Gen. 261 (2004) 109–118.
[12] J.L.H. Chau, Y.S.S. Wan, A. Gavriilidis, K.L. Yeung, Chem. Eng. J. 88 (2002) 187–200.
[13] S.M. Lai, C.P. Ng, R. Martin-Aranda, K.L. Yeung, Micropor. Mesopor. Mater. 66 (2003) 239–252.
[14] W.J. Kim, T.J. Kim, W.S. Ahn, Y.J. Lee, K.B. Yoon, Catal. Lett. 91 (1997) 123–127.
[15] K.T. Jung, Y.G. Shul, Micropor. Mesopor. Mater. 21 (1998) 281–288.
[16] K.T. Jung, Y.G. Shul, Chem. Mater. 9 (1997) 420–422.
[17] K.T. Jung, J.H. Hyun, Y.G. Shul, AIChE J. 43 (1997) 2802–2808.
[18] Y. Lee, W. Ryu, S.S. Kim, Y. Shul, J.H. Je, G. Cho, Langmuir 21 (2005) 5651–5654.
[19] Y.K. Hwang, J. Chang, S. Park, D.S. Kim, Y. Kwon, S.H. Jhung, J. Hwang, M.S. Park, Angew. Chem. Int. Ed. 44 (2005) 556–560.
[20] J. Motuzas, S. Heng, P.P.S.Z. Lau, K.L. Yeung, Z.J. Beresnevicius, A. Julbe, Micopor. Mesopor. Mater. 99 (2007) 197–205.
[21] J. Motuzas, A. Julbe, R.D. Noble, A.V.D. Lee, Z.J. Beresnevicius, Micropor. Mesopor. Mater. 92 (2006) 259–269.
[22] L.T.Y. Au, J.L.H. Chau, C.T. Ariso, K.L. Yeung, J. Membr. Sci. 183 (2001) 269–291.
[23] J.L.H. Chau, C. Tellez, K.L. Yeung, K. Ho, J. Membr. Sci. 164 (2000) 257–275.
[24] X.F. Zhang, H.O. Liu, K.L. Yeung, Mater. Chem. Phys. 96 (2006) 42–50.
[25] E.S.M. Lai, L.T.Y. Au, K.L. Yeung, Micropor. Mesopor. Mater. 54 (2002) 63–77.
[26] J. Hedlund, S. Mintova, J. Sterte, Micropor. Mesopor. Mater. 28 (1999) 185–194.
[27] G. Xomeritakis, A. Gouzinis, S. Nair, T. Okubo, M. He, R.-M. Overney, M. Tsapatsis, Chem. Eng. Sci. 54 (1999) 3521–3531.
[28] X.F. Zhang, H.O. Liu, K.L. Yeung, Carbon 44 (2006) 501–506.
[29] L.T.Y. Au, K.L. Yeung, J. Membr. Sci. 194 (2001) 33–55.
[30] W.C. Wong, L.T.Y. Au, P.S. Lau, C. Tellez, K.L. Yeung, J. Membr. Sci. 193 (2001) 141–161.
[31] L.T.Y. Au, W.Y. Mui, P.S. Lau, C.T. Ariso, K.L. Yeung, Micropor. Mesopor. Mater. 47 (2001) 203–216.
[32] C.S. Cundy, J.O. Forrest, R.J. Plaisted, Micropor. Mesopor. Mater. 66 (2003) 143–156.
[33] C.S. Cundy, J.O. Forrest, Micropor. Mesopor. Mater. 72 (2004) 67–80.
[34] M.C. Lovallo, A. Gouzinis, M. Tsapatsis, AIChE J. 44 (1998) 1903–1913.
[35] F.R. Qiu, X.B. Wang, X.F. Zhang, H.O. Liu, S.Q. Liu, K.L. Yeung, Chem. Eng. J. 147 (2009) 316–322.
[36] J. Hedlund, O. Öhrman, V. Msimang, E.V. Steen, W. Böhringer, S. Sibya, K. Möller, Chem. Eng. Sci. 59 (2004) 2647–2657.
[37] Q. Li, J. Hedlund, J. Sterte, D. Creaser, A.-J. Bons, Micropor. Mesopor. Mater. 56 (2002) 291–302.
[38] W.C. Wong, L.T.Y. Au, C.T. Ariso, K.L. Yeung, J. Membr. Sci. 191 (2001) 143–163.
[39] A. Carati, C. Flego, D. Berti, R. Millini, C. Perego, B. Stocchi, C. Perego, Stud. Surf. Sci. Catal. 125 (1999) 45–52.
[40] A. Thangaraj, M.J. Eapen, S. Sivasanker, P. Ratnasamy, Zeolites 12 (1992) 943–949.
[41] D.P. Serrano, M.A. Uguina, G. Ovejero, R. Van Grieken, M. Camacho, Micropor. Mater. 4 (1995) 273–282.
[42] N.G. Vayssilov, Catal. Rev. Sci. Eng. 39 (1997) 209–251.
[43] M. Bandyopadhyay, A. Birkner, M.W.E. Van den Berg, K.V. Klementiev, W. Schmidt, W. Grunert, H. Gies, Chem. Mater. 17 (2005) 3820–3829.
[44] T. Blasco, M.A. Camblor, A. Corma, J. Pérez-Pariente, J. Am. Chem. Soc. 115 (1993) 11806.
[45] Y.G. Li, Y.M. Lee, J.F. Porter, J. Mater. Sci. 37 (2002) 1959–1965.
[46] R.B. Khomane, B.D. Kulkarni, A. Paraskar, S.R. Sainkar, Mater. Chem. Phys. 76 (2002) 99–103.
[47] X.S. Wang, X.W. Guo, Catal. Today 51 (1999) 177–180.
[48] K. Yube, M. Furuta, N. Aoki, K. Mae, Appl. Catal. A: Gen. 327 (2007) 278–286.
[49] R. Klaewkla, S. Kulprathipanja, P. Rangsunigit, T. Rirksomboon, W. Rathbun, L. Nemeth, Chem. Eng. J. 129 (2007) 21–30.
[50] R. Klaewkla, T. Rirksomboon, S. Kulprathipanja, L. Nemeth, P. Rangsunigit, Catal. Commun. 7 (2006) 260–263.
[51] H. Liu, G. Lu, Y.L. Guo, Y. Guo, Appl. Catal. A: Gen. 293 (2005) 153–161.
[52] Y.S.S. Wan, J.L.H. Chau, A. Gavriilidis, K.L. Yeung, Chem. Commun. (2002) 878–879.
[53] Y.S.S. Wan, J.L.H. Chau, K.L. Yeung, A. Gavriilidis, J. Catal. 223 (2004) 241–249.
[54] Y.S.S. Wan, A. Gavriilidis, K.L. Yeung, Chem. Eng. Res. Des. 81 (2003) 753–760.
[55] Y.S.S. Wan, K.L. Yeung, A. Gavriilidis, Appl. Catal. A: Gen. 281 (2005) 285–293.
[56] W.T. Wong, Y.S.S. Wan, K.L. Yeung, A. Gavriilidis, Stud. Surf. Sci. Catal. 158A & B (2005) 2081–2088.
[57] Y. Wang, M. Lin, A. Tuel, Micropor. Mesopor. Mater. 102 (2007) 80–85.
[58] R. Klaewkla, T. Rirksomboon, S. Kulprathipanja, L. Nemeth, P. Rangsunvigit, Catal. Commun. 7 (2006) 260–263.
[59] G. Li, X.S. Wang, H.S. Yan, M. Liu, Y.H. Liu, Y.Y. Chen, Chin. J. Catal. 22 (2001) 465–468.
[60] X.W. Guo, X.S. Wang, M. Liu, G. Li, Y.Y. Chen, J.H. Xiu, J.Q. Zhuang, W.P. Zhang, X.H. Bao, Catal. Lett. 81 (2002) 125–130.
[61] G. Li, X.S. Wang, H.S. Yan, Y.H. Liu, X.W. Liu, Appl. Catal. A: Gen. 236 (2002) 1–7.
[62] G. Bellussi, V. Fattore, Stud. Surf. Sci. Catal. 69 (1991) 79.
[63] B. Notari, Stud. Surf. Sci. Catal. 60 (1991) 343.
[64] C.B. Khouw, H.X. Li, C.B. Dartt, M.E. Davis, in: S.T. Oyama, J.W. Hightower (Eds.), Catalytic Selective Oxidation, ACS, Washington DC, 1993, p. 273.
[65] C.B. Khouw, M.E. Davis, J. Catal. 151 (1995) 77–86.
[66] A. Tuel, S. Moussa-Khouzami, Y. Ben Taarit, C. Naccache, J. Mol. Catal. 68 (1991) 45–52.
[67] S.M. Lai, R. Martin- Aranda, K.L. Yeung, Chem. Commun. 2 (2003) 218–219.
[68] W.N. Lau, K.L. Yeung, R. Martin- Aranda, Micropor. Mesopor. Mater. 115 (2008) 156–163.